Progress In Electromagnetics Research C, Vol. 132, 89–102, 2023

Machine Learning Classification of Human Osseous Tissue through Microwave Sensing

Shilpi R. Kerketta* **and Debalina Ghosh**

Abstract—Globally, microwave frequencies are being extensively employed in numerous biomedical implementations due to its high resolution, reasonable penetration through the human tissue, and cost-effectiveness. However, the quantization of human osseous tissue through microwave sensing is still not proficient. Therefore, this article provides an insight on the prediction of onset and progression of osteoporosis developed through the use of a microwave setup for the contactless evaluation of osteoporosis. This microwave setup comprises a human wrist model as a device under test which is illuminated through a pair of planar stubbed monopole antennas to characterize the different degrees of osteoporosis through frequency domain simulation analysis. By diversifying the wrist dimensions, we are collecting the dataset of the transfer characteristics. Furthermore, different machine learning algorithms are employed on this dataset to train, classify, and eventually evaluate the different degrees of osteoporosis. Finally, an optimum machine learning algorithm was obtained to work at an optimum bandwidth and optimum frequency.

1. INTRODUCTION

Currently, bone health is a universal health issue, with a worldwide estimate of 200 million people being affected by osteoporosis-cognate fractures requiring expensive treatment. An epidemiological investigation has predicted a significant escalation in osteoporotic fractures over the next few years, [1]. This calls for an effective method for bone health analysis, which can classify the bone tissues by the degree of mineralization. The standard methodologies such as dual energy X-ray absorptiometry (DEXA), quantitative Computed tomography (QCT), quantitative ultrasound (QUS), and magnetic resonance imaging (MRI) are currently in use for the evaluation of bone mineral density (BMD). As pointed out in previous researches, DEXA is one of the most prominent methods used for estimating BMD; however, it does not offer a detailed understanding of bone quality and bone structure. Also, both DEXA and QCT are dependent on ionizing waves which could lead to health hazards and enhance cancer risks. Along with the MRI, these methods are expensive, non-portable, and time-consuming. Although QUS uses non-ionizing radiation and is portable, it causes strong reflections and cannot penetrate through the bones, and hence is less accurate [2–4].

On the other hand, based on the ever-growing applications of microwave techniques in health care, it is intuitive that microwave systems have the ability to address the challenges of bone health evaluation. Microwave systems are based on non-ionizing electromagnetic waves and are non-invasive in nature. Microwave frequencies demonstrate good penetration capability into all types of human tissues, particularly into the bones. The resolution of the microwave signal is precise enough to record minute changes in the tissue properties. Thus, the electromagnetic properties of bone tissue extracted from the reflected and/or transmitted signal can be used for bone health analysis and classification. Upon analyzing the electrical characteristics of the return signal, the dielectric characteristics of biological

Received 20 February 2023, Accepted 10 April 2023, Scheduled 16 April 2023
* Corresponding author: Shilpi Ruchi Kerketta (srk10@iitbbs.ac.in).
The authors are with the School of Electrical Sciences, IIT Bhubaneshwar, Odisha, India.

tissues can be estimated, and based on this a precise assessment and cognizance of the properties of bone health can be made.

The widespread application of machine learning algorithms in the field of signal processing has led to many advancements in health care. Many ailments can be diagnosed on a real-time basis through training and testing using machine learning algorithms. This can also shorten time-intensive and computationally expensive procedures. In the light of the recent success of machine learning in health care diagnostics, it is anticipated that similar processing will provide further light into the classification of bone health [5–7].

A currently used fracture risk assessment tool, FRAX [8, 9], is a prototype that has implemented twelve input quantities such as age, weight, sex, height, past fracture history, family fracture record, use of glucocorticoids, rheumatoid arthritis, secondary osteoporosis, alcohol consumption, and smoking. Its output product, the ten-year probability of fracture, has received some criticism.

A number of studies were done between 2001 and 2017 [10–13] which utilized one of the medical decision parameters known as osteoporosis self-assessment tool (OST) which is a simple formula-based methodology that utilized age and the human body weight as input parameters. These studies applied various machine learning algorithms such as support vector machine (SVM), random forest (RF), artificial neural network (ANN), and linear regression (LR). The limitation of this decision tool is its low accuracy.

Wang et al. in 2018 [14] predicted the risk of hip fracture in postmenopausal women implementing an artificial neural network. In the same year, Rivas et al. [15] studied the risk factor analysis of BMD as predicated by selecting type 2 diabetes.

Krishnaraj et al. in 2019 [16] used an optimized SVM analysis in biological data sets with lower density. Fathima et al. in 2020 [17] analyzed the sagittal view of CT spine images implementing a deep learning approach. Here the multiclass segmentation approach was predicated on cascaded 2 U-nets. Specificity, sensitivity and accuracy of the networks are quantized. In the same year, Recenti et al. did two different works. The first one [18] was based on a deep learning method on the segmentation of bone for BMD quantization from DEXA scan images, and the other was through a regression technique to evaluate the BMD of patients suffering from total hip arthroplasty employing Gait analysis [19].

Further Minonzio et al. in 2020 [20] created an automatic classification of patients suffering from non-traumatic fractures characterized by the ultrasonic guided wave spectrum image implementing a dynamic SVM.

A flowchart of the microwave-based analyzer model using machine learning is demonstrated for bone health evaluation (see Figure 1). It utilizes a pair of planar stubbed monopole antennas placed at an optimized distance to get the transfer characteristic.

After data-collection using the previously described microwave sensing system, the data is used for training the classifiers of the machine learning tool. During the dataset creation, the different stages of osseous tissues are simulated by varying the electromagnetic parameters of the tissues. To create a more realistic scenario in terms of variation of subject body tissue dimensions, each tissue size is varied during the simulation using the high-frequency simulation software. The transfer characteristic responses are recorded, and a dataset is created. For better estimation of the different degrees of osteoporosis, these datasets are further analyzed with the help of different machine learning algorithms. The dataset is subjected to training and testing in order to successfully classify the bone health condition. Various predictive models such as Decision Tree, Random Forest, and SVM are employed for the detection of outbreaks and advancement of osteoporosis from the information gathered through microwave analysis.

Another important step in the process of bone health classification is to be able to identify the optimum frequency range of operation. In the research work, a wideband system has been used for analysis. However, narrow-band systems often have an advantage over wideband counterparts in terms of cost and ease of design. Hence, this article looks at the prospect of using a narrow-band system for bone health analysis. This is achieved by using the prediction algorithms to identify the optimum frequency range at which the classification system has the highest accuracy.

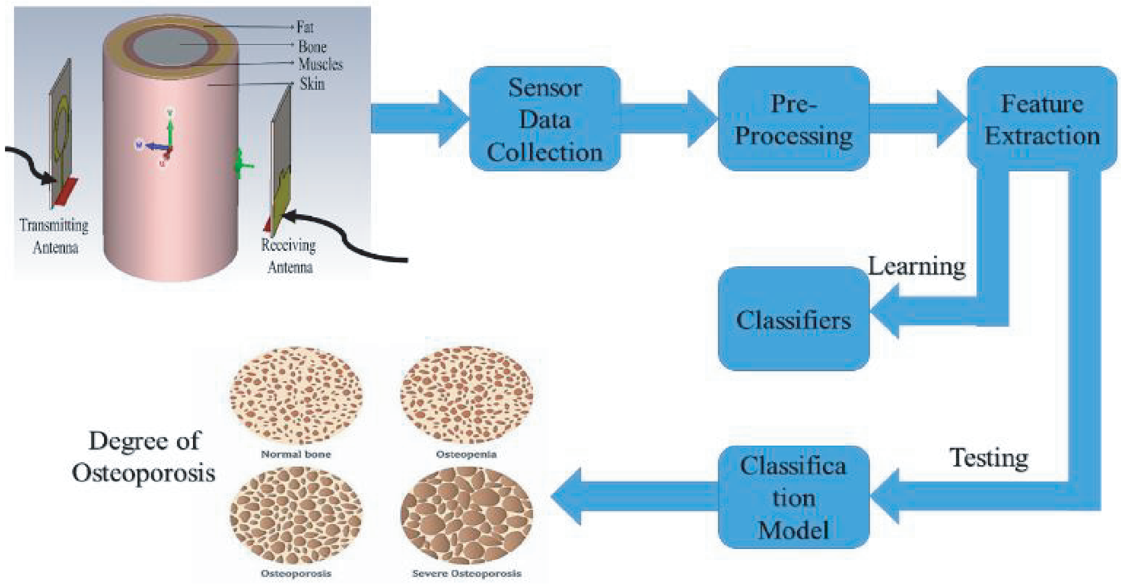

Figure 1. Flowchart for microwave sensing for bone health evaluation through machine learning.

2. ELECTROMAGNETIC SENSING BEHAVIOR OF HUMAN OSSEOUS TISSUE

2.1. UWB Stubbed Planar Monopole Antenna

In this research, the prediction of bone quality is evaluated using a ultra-wideband (UWB) microwave system. Here, a pair of circular stubbed planar monopole antennas have been proposed as illustrated in [2]. The structure of a stubbed monopole antenna comprises a circular radiating structure along with a circular slot, a $50\,\Omega$ microstrip line, and a modified stub in the partial ground plane. Here Rogers 5880 LZ substrate is chosen as substrate material having a relative permittivity of 1.98, thickness of 1.016 mm, length of 30 mm, and width of 40 mm.

The partial ground plane has a rectangular geometry with a rectangular stub integrated on the upper edge of the ground plane resulting in the enhancement of bandwidth and gain with compact size. The substrate was culled such that it can be easily integrated with cloths and had low E-field loss and low moisture absorption.

Figure 2 shows a photograph of the fabricated prototype of the proposed monopole antenna with a protruding stub. Figure 3 exhibits the comparison between the reflection coefficients of the simulated and measured monopole stubbed antennas. In accordance with the measured results, the frequency bands of the simulated and measured antennas range from 3 to 24 GHz. However, in this methodology, the operating frequency range has been limited to 3 to 8 GHz as higher frequencies have exhibited lower penetration capability towards human tissue [3].

2.2. Electromagnetic Sensing Behavior

The proposed microwave sensing technique presented here for bone mineral density evaluation employs a pair of planar stubbed monopole antennas as described in the previous studies [2]. The reason that the human wrist model was chosen as the object under test is that it is considered the most prominent location to test osteoporosis. Also, the wrist is the most prominent area where the early signs of osteoporosis can be easily diagnosed. Here the volume of the bone tissue is more than other human tissues especially compared to the muscle tissue. It is noted that muscle tissue has high permittivity and hence attenuates most electromagnetic signals allowing very low energy to pass through. The electrical and structural parameters of the human tissues are derived from the previous studies utilizing microwave sensing [21] as elaborated in [3, 4]. For the dielectric features of healthy bones, skin, fat, and

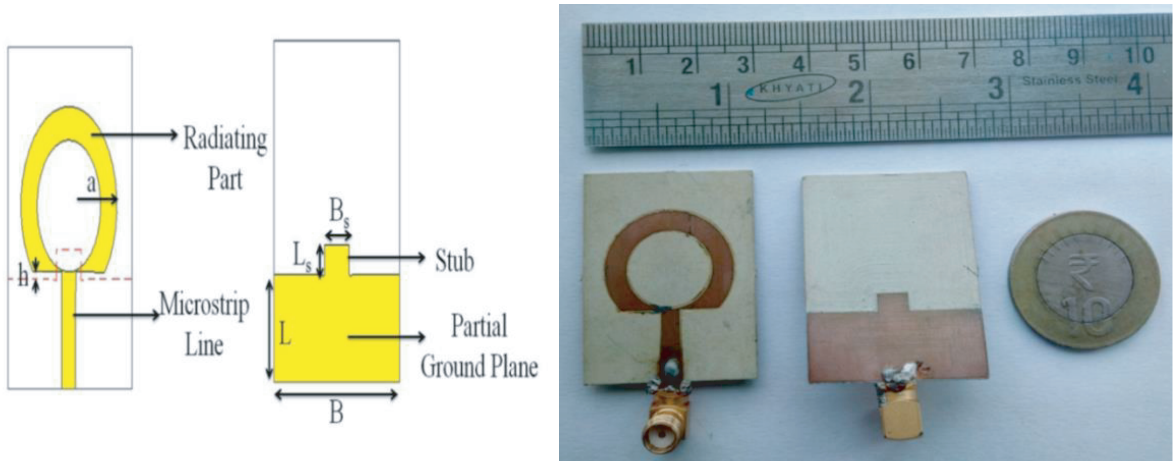

Figure 2. (a) The geometry of the stubbed ground plane monopole antenna. (b) Fabricated design of stubbed ground plane monopole antenna.

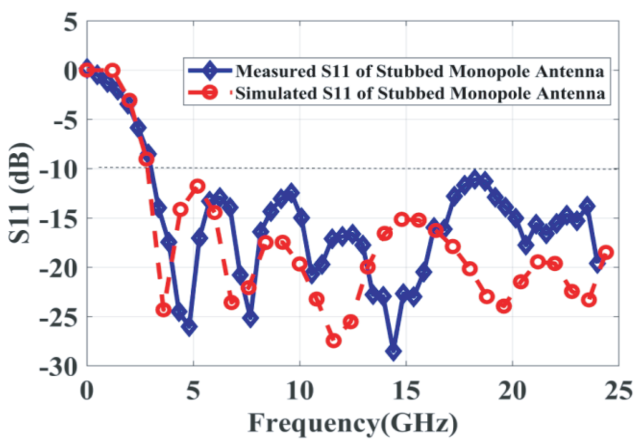

Figure 3. Comparison of the simulated and measured return loss characteristics of the stubbed ground plane monopole antenna.

muscles in built bio-tissue characteristics in the CST Microwave studio simulation software, dielectric properties of biological tissues database from the Italian national research council were taken into consideration [22, 23]. The various parameters of the osteopenia and osteoporotic bones chosen for the analysis at 6.3 GHz from the previous study [21] are listed in Table 1. In previous studies [3, 4], the analysis was focused on the temporal domain and spectral attenuation through human osseous tissue, and a statistical approach was employed to characterize the progress of osteoporosis. To increase the accuracy of the proposed system, the analysis is further enriched through the usage of a machine learning-based classifier. For the classification of the human osseous tissue, six different stages of osteoporosis are considered in a methodology as adopted in Table 1.

2.3. SAR Analysis

The radiation requirement can be estimated through Specific Absorption Rate (SAR) which is the standard methodology for the estimation of absorption of electromagnetic power by the human tissue. Here, the SAR computation is done through the stubbed planar monopole antenna and the human wrist

Table 1. Electrical properties of human tissue at 6.3 GHz.

Tissue	Relative Permitivity (Er)	Loss Tangent	Conductivity (S/m)	Radius (mm)
Healthy Bone	9.4543	0.38487	1.2772	15
Osteopenia Bone	14	0.2040	1	15
Osteoporotic Bone 1	18	0.2374	1.5	15
Osteoporotic Bone 2	23	0.2488	2	15
Osteoporotic Bone 3	28	0.275129	2.7	15
Osteoporotic Bone 4	32	0.30315	3.4	15
Muscle	47.801	0.33267	5.5818	4
Fat	4.9087	0.18965	0.32677	6
Skin	34.683	0.3424	4.1684	2

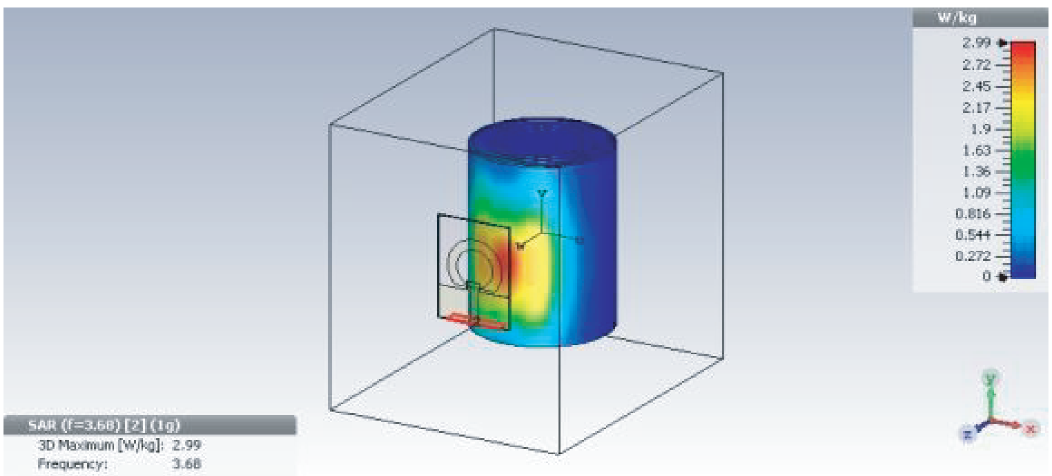

Figure 4. Maximum SAR analysis of the stubbed monopole antenna at 3.68 GHz for 1 gm of tissue.

in CST microwave studio. Figures 4–6 represent the SAR distribution over the human wrist model. The average value of SAR must be within 4 W/kg for 1 gm of tissue for human wrist. The maximum SAR value observed for 1 gm of the tissue was 2.99 W/kg, 3.01 W/kg, and 3.05 W/kg for 3.68 GHz, 5 GHz, and 7 GHz, respectively. This SAR value is calculated for 1 Watt of input power which is within the specific limit.

3. DATA COLLECTION AND FEATURE EXTRACTION

The microwave-based bone sensing was conducted with the help of high-frequency simulation software through frequency domain analysis from 3 GHz to 8 GHz. The transfer characteristics are recorded using the wideband antenna, and it is analyzed for human tissues with six different degrees of osteoporosis for standard wrist dimensions. The transfer characteristics are illustrated in Figure 7. It was observed that as the bone mineral density decreases, the first resonance appears lower in the frequency scale as there is an increase in electric permittivity and the conductivity of the bone, as illustrated in Table 1. The advantage of implementing extremely wideband antennas is that we could employ any suitable wideband which shows the most deviation and can easily differentiate between the different degrees of BMD. Apparently, through transfer characteristics simulation result in Figure 7 of this paper, we observe that

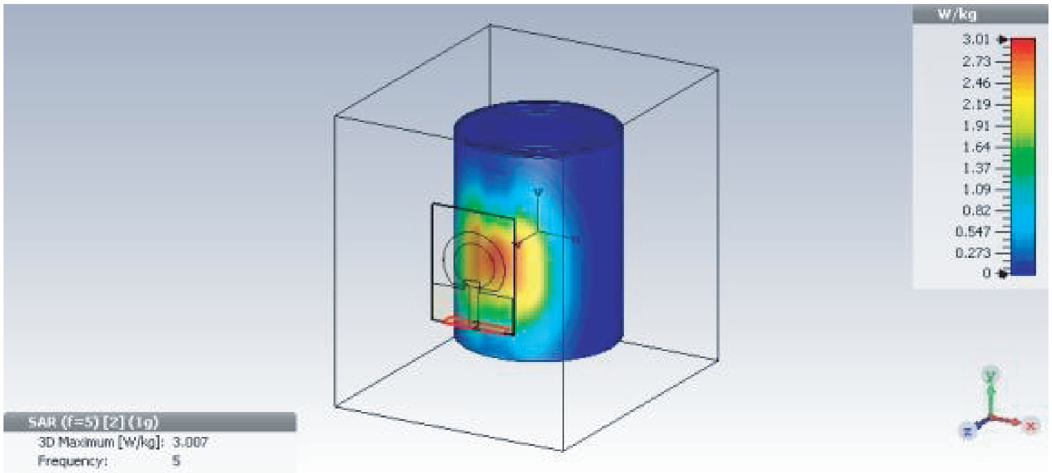

Figure 5. Maximum SAR analysis of the stubbed monopole antenna at 5 GHz for 1 gm of tissue.

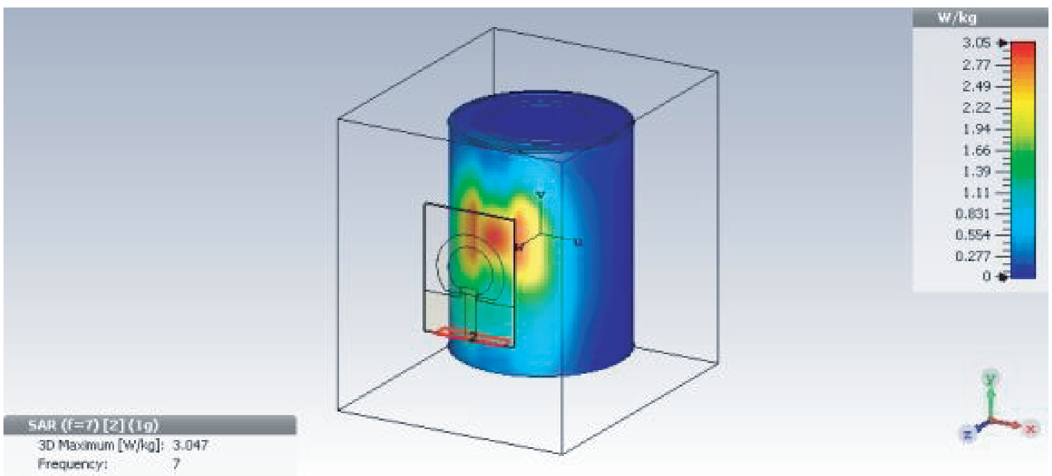

Figure 6. Maximum SAR analysis of the stubbed monopole antenna at 7 GHz for 1 gm of tissue.

after 7.5 GHz the S_{21} characteristics for different bone mineral density tend to merge showing very little deflection and fully merges at 8 GHz. So eventually, we chose a 3–8 GHz frequency band that showed a maximum and clear deflection. Each human subject may have different wrist sizes with different radial dimensions of three tissues at the wrist. The transfer characteristics will obviously deviate even with a slight alteration of the tissue dimensions. For demonstrating the proposed methodology with respect to realistic test subjects, it is essential to consider such minor dimensional variations as part of the system design. In order to address this variation, the dataset of transfer characteristics is generated by varying the different radial dimensions of tissues while at the same time varying the electromagnetic parameters of bone tissues. While creating the dataset, each human tissue such as the bone, fat, and muscle was changed individually by 0.1 mm till the radial dimension increased by 1 mm. This was repeated incorporating bone tissue with the six degrees of osteoporosis as tabulated in Table 2. This process is able to generate a total of 186 cases of transfer characteristics over 1000 individual frequency ranges between 3 and 8 GHz.

For reference purposes, a few snapshots from the collection of 186 sets of data of transfer characteristics is shown plotted in Figures 8 to 10 over the complete reference measurement frequency range of 3 GHz to 8 GHz. Each of the characteristic plots shows the variation in attenuation levels with

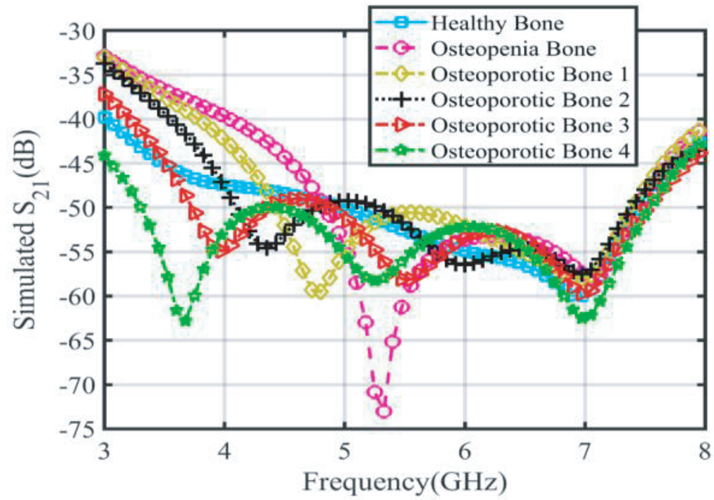

Figure 7. Through bone signal of the simulated wrist for standard dimension.

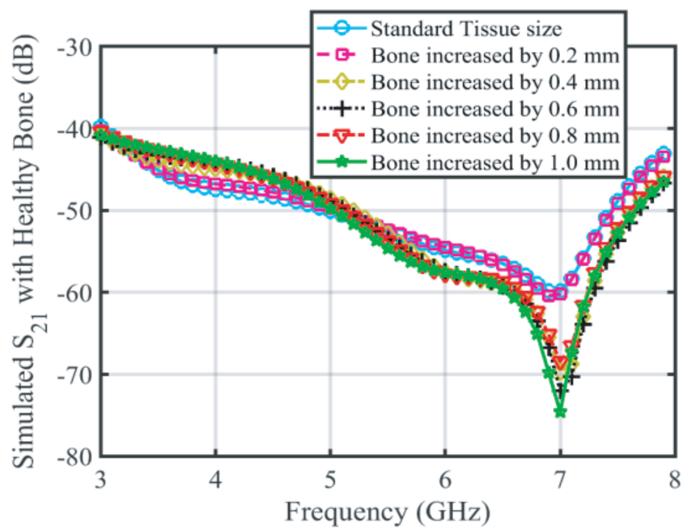

Figure 8. Through bone signal of the healthy bone by varying the bone tissue.

Table 2. Database description.

Degree/stages of osteoporosis (healthy bone, osteopenia bone, osteoporotic bone 1, 2, 3, 4)	6
Types of human tissue (fat, muscle, bone)	3
Number of deviation of each individual tissue (0.1 mm to 1 mm)	10
Number of initial readings with standard wrist dimensions	6
Total number of readings of transfer characteristics	$6 \times 3 \times 10 + 6 = 186$

the alteration in the dimensions of a particular chosen human tissue. This is in contrast to Figure 7, wherein the variable was the degree of osteoporosis, and the tissue dimension was maintained constant during the investigation. Hence, each of Figures 8 to 10 shows that even with a slight change in the

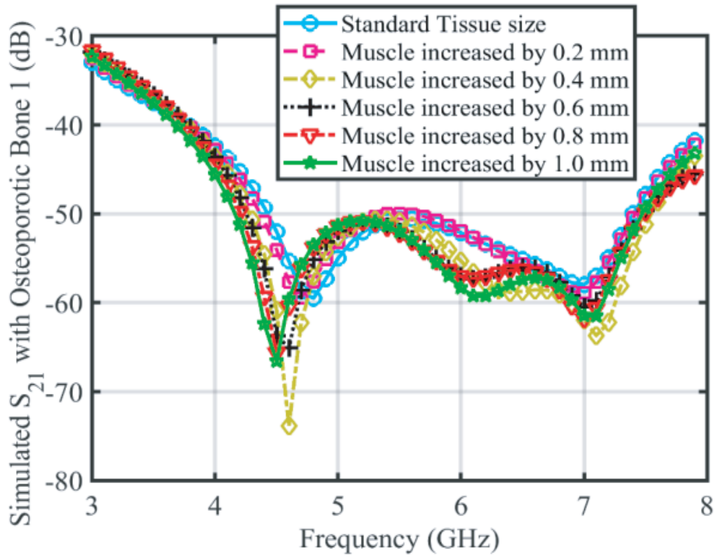

Figure 9. Through bone signal of the osteoporotic bone 1 by varying the muscle tissue.

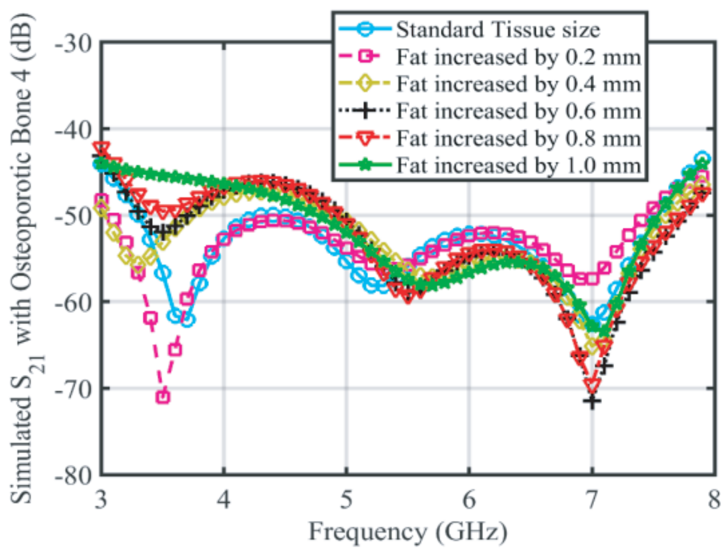

Figure 10. Through bone signal of the osteoporotic bone 4 by varying the fat tissue.

tissue dimension there is a significant variation in the transfer characteristics. It can be deduced that the determination of osteoporosis and its advancement becomes dependent on the human subject chosen.

This dependency may render the recognition of osteoporosis advancement invalid. In other words, a uniform diagnostic mechanism may fail to deliver accurate results unless the tissue variation is factored into the processing stage.

To address this non-osseous variable, it is proposed to train the classifier to identify this variation from among the collected dataset with the implementation of machine learning algorithms. Due to the absence of an accurate classification approach, it would be tough to estimate the stage of the advancement of osteoporosis. An appropriate classification algorithm will be able to distinguish the distinct features attributable to the variation in BMD while repressing the effect of the variations in the human tissue dimensions.

4. IMPLEMENTATION OF MACHINE LEARNING ALGORITHM IN HEALTH CARE

Machine learning algorithms are formulated to combine algorithmic strategy with statistical methodology. Machine learning algorithms are recognized as a subclass of Artificial Intelligence (AI) applications [24]. They are employed by computerized systems for implementing a function without utilizing definitive instructions. Properly trained, they are able to do the job with accuracy identifying pinpointed intrusions and delicate patterns. The health care diagnostic instruments are highly dependent on the accuracy and time-effectiveness of the adopted technology. So the implementation of the machine learning algorithms for computer-aided diagnosis enables the system for rapid analysis and enhances the diagnostic accuracy at the same time [25]. A few of the machine learning algorithms in a particular random forest, decision trees, and support vector machines (SVMs) which have distinct advantages in terms of building a prediction model with the basic form of datasets [26] are detailed here.

4.1. Decision Tree Induction

Decision trees are broadly acknowledged as a machine learning and data mining approach that undertakes an attribute value dataset as the input and develops Boolean decisions the output. It consists of a tree where each individual node is depicted as a test attribute and each leaf node depicted as classification. The test example classification starts at the root, then each node is tested according to the attribute values of each individual node and followed by the sorting of branch appropriately until it attains the appropriate leaf node classification. Here, the training set is divided in accordance with the relevant values of the selected nodes through these branches, and the decision tree algorithm is implemented recursively to each dataset [27]. It gives optimal results if the dataset is adequately classified and consists of the least number of nodes. The accuracy generated through this method is high, but it also has the disadvantage of excessive complications [28].

4.2. Random Tree

The fundamental idea of the random forest algorithm is the incorporation of several decision tree classifier models. It can be explained as that the combination of random subspace and bagging creates decisions and produces a final output by voting through decision making. The procedure of the random forest algorithm is split into two important sections, firstly towards the growth of the decision tree and secondly towards the voting on the procedure. In particular, the growth procedure is again separated into three features such as randomly selecting the training dataset, construction of random forest, and splitting up the nodes. The final prediction is made by aggregating the decisions developed by trees in the forest [29–31].

4.3. Support Vector Machine

Support vector machines are some of the supervised learning models which are associated with machine learning algorithms that can analyze the data and figure out the patterns, and they are utilized in the regression and classification analysis. Originally, SVM was established to solve the binary problems based on classification, which employed a hyper-plane that acted as a decision boundary separating the data point from distinct classes [32]. These can manage both linear, simple classification operations and nonlinear, more complex, classification problems. They can handle both distinguishable and non-distinguishable problems in linear and nonlinear tasks.

The basic notion of SVM is to project the data points from the original input space towards a high or infinite-dimensional feature space in such a way that the classification task seems simplified in the feature space. The mapping is created through the most appropriately selected kernel function. The fundamental distinction between the SVM and other conventional algorithms is that it employs the structural risk minimization (SRM) technique and opposes the empirical risk minimization (ERM) technique which is extensively utilized in statistical training. Generally, the SRM attempts to diminish the upper bound on the generalization instead of diminishing the training error which is expected to have better efficiency than the traditional ERM technique. Additionally, SVM consists of convex optimization, which particularly assures that the local minimization is a distinctive minimization [33, 34].

5. CLASSIFICATION AND VERIFICATIONS

The machine learning algorithms were implemented utilizing Python programming language. Three classification models were built using the decision tree, random forest, and support vector machine algorithms on the dataset of transfer characteristics described in Section 3. The classification report is generated by training using 60% of the dataset and using the rest 40% of the dataset for testing [35, 36]. Table 3 illustrates the classification report using different machine learning algorithms in terms of accuracy and confusion matrix. While the 6 different cases of osteoporotic bone tissues are classified, the accuracy for the decision tree is 91%; random forest is 95%; and for SVM it is 97%. Further, the precision, recall, f1-score, and support parameters for the employed classifiers are detailed in Table 4 for each of the machine learning algorithms. This outcome is very encouraging, particularly because of the high accuracy achieved even in the presence of significant variation in the dataset due to unaccounted variations in the tissue dimensions chosen.

Table 3. Report on bone health classification over a frequency band of 3–8 GHz.

ML Algorithms	Random Forest	Decision Tree	Support Vector Machine
Confusion Matrix	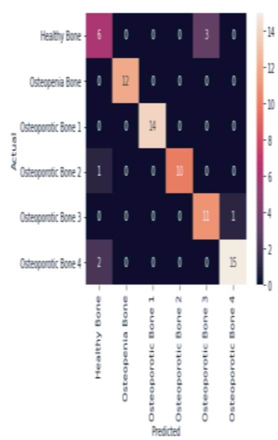	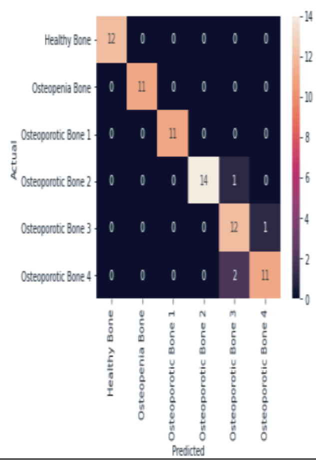	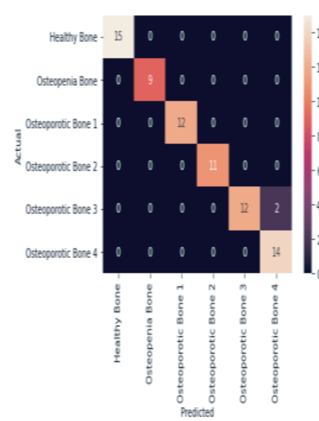
Accuracy	91%	95%	97%

It may be noted that the classifiers were employed on the raw data collected from the microwave sensing system, and further feature extraction may be utilized in the future to increase the accuracy while reducing the training complexity.

The above procedure has been employed on wideband sensor data. However, as pointed out it is worthwhile to investigate the frequency dependence on the accuracy of the model. This can help in focusing on the frequency range with higher accuracy and be able to use a narrow-band system.

For this purpose, the frequency band of 3–8 GHz was subdivided into 1 GHz bands. The original 3–8 GHz band consisted of 1000 frequency samples. After subdivision into 1 GHz bands, each of the datasets consists of 186 transfer characteristics with each measured at 200 distinct frequencies. This results in the creation of 5 independent datasets which are next fed into the machine learning algorithms for training and testing as described previously. The classification result is detailed in Table 5.

It is observed that for each of the machine learning algorithms employed the system accuracy varies depending on the frequency band chosen. For the decision tree algorithm, the system is most accurate

Table 4. Report on bone health classification over a frequency band of 3–8 GHz using random forest, decision tree algorithm and support vector machine.

	Random Forest				Decision Tree				Support Vector Machine			
Tissue	precision	recall	f1-score	support	precision	recall	f1-score	support	precision	recall	f1-score	support
Healthy Bone	0.67	0.67	0.67	9	1	1	1	12	1	1	1	15
Osteopenia Bone	1	1	1	12	1	1	1	11	1	1	1	9
Osteoporotic Bone 1	1	1	1	14	1	1	1	11	1	1	1	12
Osteoporotic Bone 2	1	0.91	0.95	11	1	0.93	0.97	15	1	1	1	11
Osteoporotic Bone 3	0.79	0.92	0.85	12	0.8	0.92	0.86	13	1	0.86	0.92	14
Osteoporotic Bone 4	0.94	0.88	0.91	17	0.92	0.85	0.88	13	0.88	1	0.93	14

Table 5. Accuracy comparison bone health evaluation with diversified frequency data employed for training.

	Broadband 3–8 GHz	1 GHz Bandwidth					Single Frequency	
Total No. of frequency data	1000	200					1	
Frequency	3–8 GHz	3–4 GHz	4–5 GHz	5–6 GHz	6–7 GHz	7–8 GHz	3.485 GHz	3.62 GHz
Random Forest	91	89	**92**	80	72	72	56	**74**
Decision Tree	95	**92**	85	80	72	67	**76**	70
SVM	97	91	**96**	87	86	68	**73**	50

(92%) for a bandwidth of 4–5 GHz, and for the random forest algorithm the system shows similar levels of accuracy (92%) for frequency bands of 3–4 GHz. However, when SVM is implemented it shows a maximum accuracy of 96% for the frequency band of 3–4 GHz. In this case, the most appropriate frequency band is found to be 4–5 GHz. Though the above result shows some variation, it does point to the fact that frequencies in the lower ranges up to 6 GHz carry more information regarding the tissue characteristics than the frequencies higher than 6 GHz. This definitive understanding is crucial to the future system design of microwave-based bone health diagnostic systems.

On the basis of the above findings, a further investigation was carried out to identify the effectiveness of a single frequency band system for the classification process. The frequency band of 3–5 GHz was chosen, and the machine learning algorithms were employed on individual frequency data in the range. By applying each of the three algorithms, it is found that the system is most accurate at 3.485 GHz for both random forest and SVM algorithms with the accuracy of 74% and 73%, respectively. For the decision tree, it is found that the system is most accurate at 3.62 GHz with 74% accuracy. It is noted that there is a clear fall in the accuracy of the classification process when a single frequency evaluation is carried out. This is likely due to the lack of sufficient data points in the dataset created for single-frequency evaluation. It is well known that the accuracy of the machine learning classifier is heavily dependent on the availability of a large dataset for training the classifier. Hence, the above results indicate that a single frequency setup may not be the most appropriate solution under this scenario. At the same time, this procedure allows us to fine-tune our system highlighting the most appropriate frequency of operation.

6. CONCLUSION

The proposed methodology presented here focuses on microwave-based sensing of bone health evaluation employing a machine learning algorithm for varying human wrist sizes. A series of simulations utilizing a pair of planar stubbed monopole antennas placed in proximity to the human wrist with varying dimensions are undertaken to create a dataset. Machine learning algorithms such as decision trees, random forest, and support vector machines have been employed on the dataset of transfer characteristics for a bandwidth of 3 to 8 GHz. It is shown that even though the size of each tissue is varied the sensor is capable of classifying six different degrees of osteoporosis with high accuracy. To further evaluate the system accuracy the bandwidth of 5 GHz is divided into 1 GHz bands, and it is shown that the frequency band of 4–5 GHz gives a good accuracy even with fewer samples in the dataset. To further find an optimum frequency single frequency-based classification is undertaken.

The human osseous tissue permittivity and conductivity are correctively related to the bone quality and bone mineral density features which include the micro-architecture and mechanical characteristics. The attenuation of electromagnetic signals through healthy bone is quite different from that of osteopenia and osteoporotic bone despite the different wrist sizes. Hence, in the practical examination, properly training and testing the dataset and implementing an appropriate machine learning algorithm can give a highly accurate prediction.

REFERENCES

1. Lin, J. T. and J. M. Lane, "Osteoporosis: A review," *Clin. Orthopaedics Relat. Res.*, Vol. 425, 126–134, 2004.
2. Kerketta, S. R. and D. Ghosh, "Bandwidth enhancement of monopole antenna using stubbed ground plane," *Wiley — Int. J. RF Microw. Comput. Aided Eng.*, Vol. 29, No. 10, e21868, 2019.
3. Kerketta, S. R. and D. Ghosh, "Microwave sensing for human bone health evaluation," *Elsevier AEU — International Journal of Electronics and Communications*, Vol. 127, 153469, 2020.
4. Kerketta, S. R. and D. Ghosh, "Microwave analysis on bone mineral density," *2020 International Symposium on Antennas & Propagation (APSYM)*, 83–86, Cochin, India, 2020.
5. Roohi, M., J. Mazloum, M. A. Pourmina, and B. Ghalamkari, "Machine learning approaches for automated stroke detection, segmentation, and classification in microwave brain imaging systems," *Progress In Electromagnetics Research C*, Vol. 116, 193–205, 2021.
6. Bamatraf, S. M., M. A. Aldhaeebi, and O. M. Ramahi, "Noninvasive continuous glucose monitoring on aqueous solutions using microwave sensor with machine learning," *Progress In Electromagnetics Research Letters*, Vol. 102, 127–134, 2022.
7. Santorelli, A., E. Porter, E. Kirshin, Y. J. Liu, and M. Popovic, "Investigation of classifiers for tumor detection with an experimental time-domain breast screening system," *Progress In Electromagnetics Research*, Vol. 144, 45–57, 2014.
8. Kanis, J. A., O. Johnell, A. Odén, H. Johansson, and E. McCloskey, "FRAX$^{\mathrm{TM}}$and the assessment of fracture probability in men and women from the UK," *Osteoporosis International*, Vol. 19, No. 4, 385–397, 2008.
9. Rubin, K. H., T. Friis-Holmberg, A. P. Hermann, B. Abrahamsen, and K. Brixen, "Risk assessment tools to identify women with increased risk of osteoporotic fracture: Complexity or simplicity?," *A Systematic Review. Journal of Bone and Mineral Research*, Vol. 28, No. 8, 1701–1717, 2013.
10. Koh, L. K., W. B. Sedrine, T. P. Torralba, A. Kung, S. Fujiwara, S. P. Chan, Q. R. Huang, R. Rajatanavin, K. S. Tsai, H. M. Park, and J. Y. Reginster, "A simple tool to identify Asian women at increased risk of osteoporosis," *Osteoporos Int.*, Vol. 12, 699–705, 2001.

11. Richy, F., M. Gourlay, P. D. Ross, S. S. Sen, L. Radican, F. D. Ceulaer, W. B. Sedrine, O. Ethgen, O. Bruyere, and J. Y. Reginster, 'Validation and comparative evaluation of the Osteoporosis Self-assessment Tool (OST) in a Caucasian population from Belgium," *QJM*, Vol. 97, 39–46, 2004.
12. Kim, S. K., T. K. Yoo, E. Oh, and D. W. Kim, "Osteoporosis risk prediction using machine learning and conventional methods," *2013 35th Annual International Conference of the IEEE Engineering in Medicine and Biology Society (EMBC)*, 188–191, Osaka, July 2013.
13. Ho-Le, T. P., J. R. Center, J. A. Eisman, T. V. Nguyen, and H. T. Nguyen, "Prediction of hip fracture in post-menopausal women using artificial neural network approach," *2017 39th Annual International Conference of the IEEE Engineering in Medicine and Biology Society (EMBC)*, 4207–4210, Seogwipo, July 2017.
14. Wang, W., B. Jiang, S. Ye, and L. Qian, "Risk factor analysis of bone mineral density based on feature selection in type 2 diabetes," *2018 IEEE International Conference on Big Knowledge (ICBK)*, 221–226, Singapore, 2018.
15. Rivas, P., S. Moore, U. Iwaniec, R. Turner, K. Grant, and E. Baker, "Optimizing support vector machine analysis in low density biological data sets," *2018 International Conference on Computational Science and Computational Intelligence (CSCI)*, 1357–1361, Las Vegas, NV, USA, 2018.
16. Krishnaraj, A., S. Barrett, O. Bregman-Amitai, M. Cohen-Sfady, A. Bar, D. Chettrit, M. Orlovsky, and E. Elnekave, "Simulating dual-energy X-ray absorptiometry in CT using deep-learning segmentation cascade," *Journal of the American College of Radiology*, Vol. 16, No. 10, 1473–1479, 2019.
17. Fathima, S. M. N., R. Tamilselvi, M. P. Beham, and A. Nagaraj, "A deep learning approach on segmentation of bone for BMD measurement from DEXA scan images," *2020 Sixth International Conference on Bio Signals, Images, and Instrumentation (ICBSII)*, 1–5, Chennai, India, October 2020.
18. Recenti, M., C. Ricciardi, K. Edmunds, M. K. Gislason, and P. Gargiulo, "Machine learning predictive system based upon radiodensitometric distributions from mid-thigh CT images," *European Journal of Translational Myology*, Vol. 30, No. 1, 2020.
19. Recenti, M., C. Ricciardi, R. Aubonnet, L. Esposito, H. Jónsson, and P. Gargiulo, "A regression approach to assess bone mineral density of patients undergoing total hip arthroplasty through gait analysis," *2020 IEEE International Symposium on Medical Measurements and Applications (MeMeA)*, 1–6, Bari, Italy, 2020.
20. Minonzio, J. G., B. Cataldo, R. Olivares, D. Ramiandrisoa, R. Soto, B. Crawford, V. H. C. De Albuquerque, and R. Munoz, "Automatic classifying of patients with non-traumatic fractures based on ultrasonic guided wave spectrum image using a dynamic support vector machine," *IEEE Access*, Vol. 8, 194752–194764, 2020.
21. Amin, B., M. A. Elahi, A. Shahzad, E. Parle, L. McNamara, and M. O'Halloran, "An insight into bone dielectric properties variation: A foundation for electromagnetic medical devices," *2018 EMF-Med 1st World Conference on Biomedical Applications of Electromagnetic Fields (EMF-Med)*, 1–2, Split, Croatia, 2018.
22. Andreuccetti, D., R. Fossi, and C. Perrucci, "Calculation of the dielectric properties of body tissues in the frequency range 10 Hz–100 GHz," *IFAC-CNR, Florence (Italy)*, 1997–2015.
23. Gabriel, C., T. Y. A. Chan, and E. H. Grant, "Admittance models for open ended coaxial probes and their place in dielectric spectroscopy," *Phys. Med. Biol.*, Vol. 39, 2183–200, 1994.
24. Zaouiat, C. E. and A. Latif, "Internet of things and machine learning convergence: The E-healthcare revolution," *Proceedings of the 2nd International Conference on Computing and Wireless Communication Systems*, 1–5, 2016.
25. Huh, J., "Big data analysis for personalized health activities: Machine learning processing for automatic keyword extraction approach," *Symmetry*, Vol. 10, No. 4, 93, 2018.
26. Sasubilli, S. M., A. Kumar, and V. Dutt, "Machine learning implementation on medical domain to identify disease insights using TMS," *2020 International Conference on Advances in Computing and Communication Engineering (ICACCE)*, 1–4, Las Vegas, NV, USA, June 2020.

27. Gavankar, S. S. and S. D. Sawarkar, "Eager decision tree," *2017 2nd International Conference for Convergence in Technology (I2CT)*, 837–840, Mumbai, India, April 2017.
28. Patil, D. V. and R. S. Bichkar, "A hybrid evolutionary approach to construct optimal decision trees with large data sets," *2006 IEEE International Conference on Industrial Technology*, 429–433, Mumbai, India, December 2006.
29. Lan, H. and Y. Pan, "A crowdsourcing quality prediction model based on random forests," *2019 IEEE/ACIS 18th International Conference on Computer and Information Science (ICIS)*, 315–319, Beijing, China, June 2019.
30. Breiman, L., "Bagging predictors," *Machine Learning*, Vol. 24, No. 2, 123–140, 1996.
31. Yi, H., Q. Xiong, Q. Zou, R. Xu, K. Wang, and M. Gao, "A novel random forest and its application on classification of air quality," *2019 8th International Congress on Advanced Applied Informatics (IIAI-AAI)*, 35–38, Toyama, Japan, July 2019.
32. Conceicao, R. C., M. O'Halloran, M. Glavin, and E. Jones, "Support vector machines for the classification of early-stage breast cancer based on radar target signatures," *Progress In Electromagnetics Research B*, Vol. 23, 311–327, 2010.
33. Wu, Y., Z.-X. Tang, B. Zhang, and Y. Xu, "Permeability measurement of ferromagnetic materials in microwave frequency range using support vector machine regression," *Progress In Electromagnetics Research*, Vol. 70, 247–256, 2007.
34. Hall, M. and G. Holmes, "Benchmarking attribute selection techniques for discrete class data mining," *IEEE Transactions on Knowledge and Data Engineering*, Vol. 15, No. 3, 1437–1447, 2003.
35. Kerketta, S. R. and D. Ghosh, "Detection of onset and progression of osteoporosis using machine learning," *Machine Learning for Healthcare Applications*, 137–149, 2021.
36. Kumar, D., A. Sarkar, S. R. Kerketta, and D. Ghosh, "Human activity classification based on breathing patterns using IR-UWB radar," *2019 IEEE 16th India Council International Conference (INDICON)*, 1–4, Rajkot, India, December 2019.